FOUNDATIONAL DATA PRODUCTS FOR THE EXPLORATION OF THE LUNAR POLAR REGIONS: IRON, OMAT AND MINERALOGY USING THE KAGUYA SPECTRAL PROFILER AND THE LUNAR ORBITER LASER ALTIMETER. M. Lemelin[1], Paul G. Lucey[2], Alex Camon[1] [1]Département de Géomatique appliquée, Université de Sherbrooke, Québec, Canada, J1K 2R1 (Myriam.Lemelin@USherbrooke.ca), [2]Hawaii Institute of Geophysics and Planetology, Department of Geology and Geophysics, University of Hawaii at Manoa, Honolulu, HI, USA.

Introduction: Investigating the composition of the polar regions is important to further our understanding of the formation and evolution of the Moon. Orbital based investigations can offer a broad regional view of the mineralogy, which can then be used to assist in either site selection for future exploration missions or in the interpretation of rover based data. However, orbital mineralogical investigations have offered limited answers so far as. As a result of the low axial tilt of the Moon with respect to the ecliptic, the VIS/NIR radiance reaches extreme lows in topographic depressions and highs on equator-facing slopes. Calibrated reflectance data, including a precise topographic correction, is thus scarse and the mineralogical identification difficult.

The first attempt to derive mineral maps in the polar region using VIS/NIR reflectance has been derived by Lemelin et al. [1]. They used the calibrated reflectance data from the Lunar Obiter Laser Altimeter (LOLA) [2] and reflectance ratio from the Kaguya Spectral Profiler (SP) [3,4] to derive the first 1 km per pixel FeO map of the polar regions. They used continuum-removed reflectance data acquired by SP during the North and South polar summers (~2000 orbits of data) and radiative transfer equations to model the mineral abundances (olivine, pyroxenes and plagioclase) of each spectrum, constrained by its abundance in FeO. Moriarty et al. later [5,6] used the Moon Mineralogy mapper (M3) data to investigate the composition of pyroxenes in the South Pole-Aitken (SPA) basin based on the position and intensity of their 1 and 2 μm bands. Recently, Blalock et al. [7] used the Kaguya Multiband Imager data and the method of Lemelin et al. [8-9] to quantify the abundance of olivine, pyroxenes and plagioclase at a spatial resolution of 60 m per pixel. Gaps in coverage occur however near the poles and at some longitudes.

Here we use the method of Lemelin et al. [1] to quantify the abundance of FeO, minerals (olivine, pyroxenes and plagioclase), nanophase iron and a new OMAT product at 1 km in the both polar regions all derived using data from the entire set of SP orbits (~8000).

Datasets: The LOLA instrument sends a laser pulse at 1064 nm and measures the energy returned from the surface at 0° phase angle, regardless of the Sun's illumination conditions [10]. It provides high signal to noise ratio for the entire lunar surface, regardless of topography, and has been thoroughly calibrated and gridded into polar maps of 1 km per pixel [2]. SP is a spot spectrometer which conducted continuous spectral observations in the VIS/NIR region (500-2600 nm) between 2007 and 2009, with ~550 m spacing between each spectrum [3,4]. Here we used SP data level 2B1, which contains radiometrically calibrated radiance data converted to diffuse reflectance. We applied the photometric function of Yokota et al. [11] to correct for the observational geometry in the 752.8 to 1555.5 nm wavelength range, and obtained the reflectance at an incidence angle of 30° and emission angle of 0°.

Methods: We used the 955.5/752.8 nm reflectance ratio from SP and calibrated reflectance at 1064 nm from LOLA to derive polar maps of FeO. We scaled the LOLA reflectance to the SP reflectance at 1064 nm to bring the LOLA data and reflectance ratio to a common viewing geometry. We reproduced the calculation of Lucey et al. [12], changing the location of the optimized origin and the iron parameter. We used the same approach to derive the OMAT parameter map [13]. To derive mineral abundances, we compared continuum-removed SP reflectance spectra between 752.8 and 1555.5 nm, to spectra we modeled using radiative transfer equations (details in [1]). We analysed SP points that have a signal-to-noise ratio >50 and a radiance >5 W/sr/m^2/nm at 752.8 and 955.4 nm. Gaps between the ~9 million reflectance measurements used in each polar region have been filled using a bilinear interpolation method following the data projection.

Results and conclusion: The new OMAT product calculated herein offers of fantastic view of the south polar region, highlighting small fresch craters, the fresh walls and central peaks of larger craters as well as high-OMAT rays extending through multiple degrees of latitude (e.g., Tycho's and de Forest). The FeO abundances are in good agreement with the abundances measured by the Lunar Propector Gamma-Ray Spectrometer [14] (r = 0.96 in the equatorial region, r = 0.78 in the polar region). The mineral abundances offer a refinement after [1]. The modeled spectra are in excellent agreement with the observed SP spectra (mean r = 0.95). The largely noritic character of the South Pole-Aitken and the increase in high-calcium pyroxene towards higher latitudes are consistent with the M3 data [5,6]. The abundance of olivine and low-calcium pyroxene are generally co-located although olivine abundances are much lower. The nanophase data shows the lowest values in SPA and in small fresh craters consistent with the OMAT data. The same products have been derived for the north polar region.

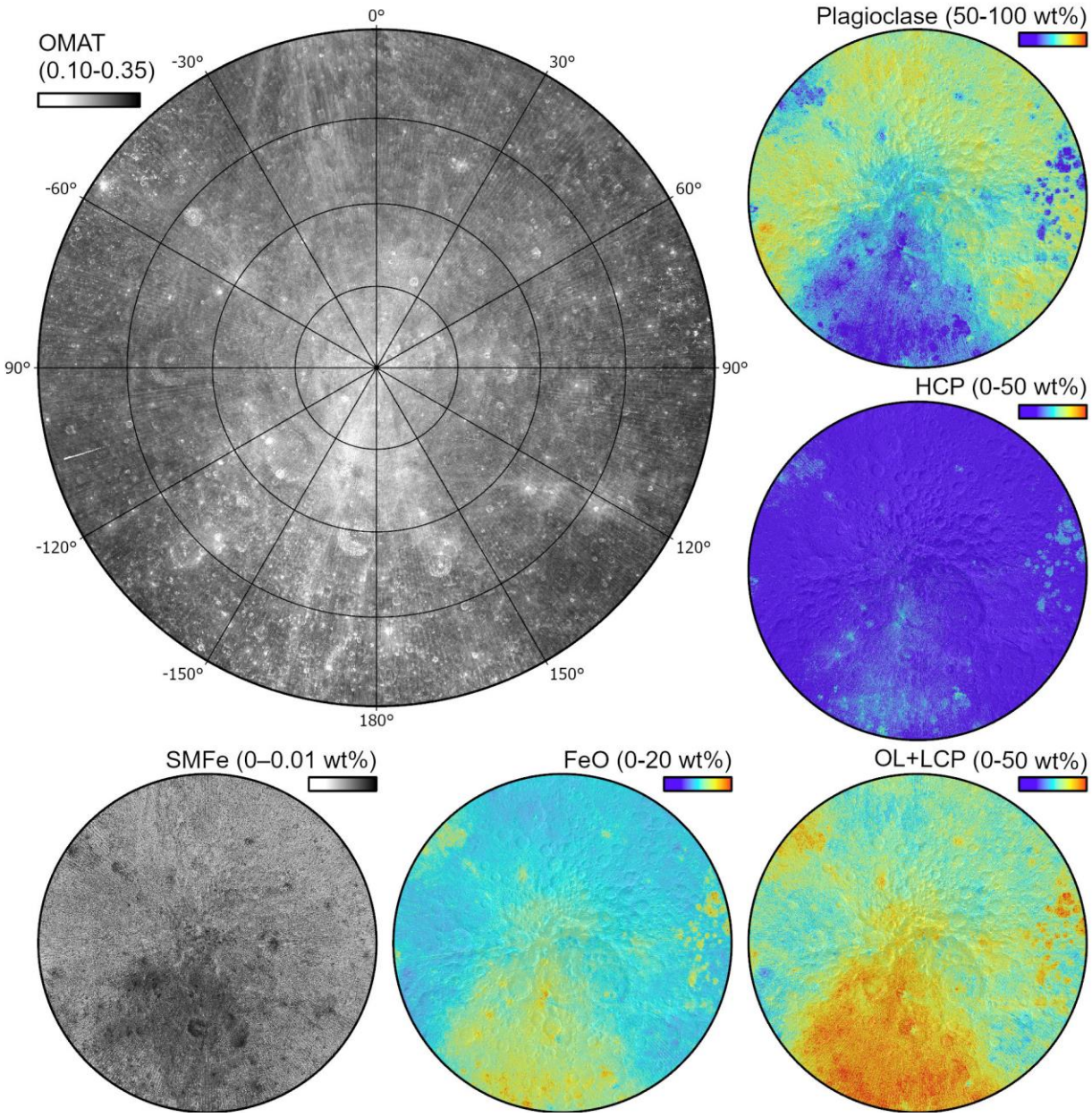

Figure 1. South polar maps of OMAT, FeO, SMFe and minerals (olivine, pyroxenes and plagioclase) derived using high signal data (~ 9M points) from the entire set of Sectral Profiler orbits and Lunar Orbiter Laser Altimeter normal albedo gridded data [4]. The abundance of olivine and low-calcium pyroxene have been merged here to simplify visualization. The data is shown in polar stereographic projection between 50-90ºS using 30% transparency over the Wide Angle Camera global mosaic.

References: [1] Lemelin M. et al. (2017) LPSC XLVIII, #2479. [2] Lemelin M. et al. (2016) *Icarus, 273*, 315-328. [3] Matsunaga T. et al. (2001) *Proc. SPIE*, *4151*, 32-39. [4] Haruyama J. et al. (2008) *EPS, 60*, 243-255. [5] Moriarty III, D.P. et al. (2018), *JGR Planets*, *123(3)*, 729-747. [6] Moriarty III, D.P. et al. (2020) *LSSW*, #5152. [7] Lemelin, M. et al. (2016) *47th LPSC*, #2994. [8] Lemelin, M. et al. (2015) *JGR, 120*, 869-887. [9] Lemelin, M. et al. (2019) *PSS, 165*, 230-243. [10] Smith D.E. et al. (2010) *Space Sci. Rev*. *150*, 209-241. [11] Yokota Y. et al. (2011) *Icarus, 215*, 639-660. [12] Lucey P.G. et al. (2000) *JGR, 105*(E8), 20,297-20,305. [13] Lucey P.G. et al. (2000) *JGR, 105*(E8), 20,377-20,386. [14] Lawrence D.J. et al. (2002) *JGR, 107(E12)*, 5130.